Vibrational Relaxation of Chemically Excited SiO ($v = 1$—5) Produced in the Reaction of Silane with O(^{1}D)

Atsuko Takahara,# Atsumu Tezaki,* and Hiroyuki Matsui

Department of Mechanical Engineering, The University of Tokyo, 7-3-1 Hongo, Bunkyo-ku, Tokyo 113-8656

(Received August 24, 1999)

The state-resolved vibrational relaxation process of SiO was monitored in the excimer laser photolysis of N_2O/SiH_4/He mixtures, where vibrationally hot SiO (T_v = 5200 K) was produced by the reaction of SiH_4+ O(^{1}D). A frequency-doubled optical parametric oscillator was used as a widely tunable source to probe SiO (v = 0—7) by the laser-induced fluorescence technique. From an analysis of the observed relaxation profiles, the vibrational transition rate constants in collisions with He and N_2O were evaluated against the vibrational level v = 1—5 of SiO. Previous theories for the V–T and V–V energy transfer were compared with the present experimental results.

Molecular vibrational energy transfer (VET) is an essential element for understanding thermal and photo-induced chemical processes.[1—3] Special attention is given to the VET of molecules having high vibrational quanta because of its importance in the unimolecular reaction and mode-selective chemistry.[1,2] Overtone excitation and stimulated emission pumping (SEP) are distinctive techniques for the aim to prepare excited molecules in a single vibrational state; however, the number of species applicable by these methods is still limited. Hence, other methods, such as chemical excitation, remain as effective tools for investigating the VET of various molecules.[4,5]

Previously, we reported the rate constant, product branching fractions and product energy distributions in the SiH_4+ O(^{1}D) reaction so as to discuss the reaction pathways of this highly exothermic, multiple-channel reaction.[6,7] A notable feature is the production of vibrationally hot SiO. It is considered to be the result of a two-step unimolecular decomposition of activated silanol formed via an insertion of O(^{1}D) into a Si–H bond of SiH_4. In this paper, state-specific VET rate constants of SiO (v = 1—5) in collisions with N_2O and He are determined by analyzing the time profiles of individual vibrational states of SiO by separating the contribution of the formation reaction. The VET mechanism is discussed by comparing the experimental results with conventional V–T and V–V transfer theories.

Experimental

Laser-photolysis with a laser-induced fluorescence (LIF) probe technique was conducted in a quasi-static flow cell. The experimental setup employed in this study was the same as that used in our previous study.[7] Briefly, mixtures of N_2O and SiH_4 diluted in He were flowed in a cell and irradiated by a 193 nm ArF excimer laser (Lambda Physik, Compex 102), where N_2O was photolyzed to produce O(^{1}D). The typical fluence of the photolysis pulse was 10 mJ cm^{-2} at the observation point.

An optical parametric oscillator (OPO; Continuum, Surelite OPO) was used as the probe light source for the LIF method. In this OPO laser, a BBO crystal was used to generate a tunable light source, and was pumped by a frequency-tripled Nd–YAG laser (Continuum, Surelite-II YAG). The "signal" was frequency doubled by another BBO crystal to generate a tunable UV pulse. For a wavelength scan, the doubling crystal and the OPO crystal were synchronously rotated by a pair of home-made PC-controlled mechanical devices. The spectral linewidth of the UV probe ranged from 4 cm^{-1} (FWHM) at 230 nm to 7 cm^{-1} at 300 nm. This width is wider than that of the typical dye lasers or narrow-band OPOs; nevertheless, it has a sufficient resolution to discriminate the progression of vibrational bands of SiO. This setup has a merit that the output can be scanned quickly over a wide range of wavelengths without changing the measurement conditions, so that the spectra of highly reproducible intensities are obtained.

Fluorescence from SiO was transmitted through a selected UV bandpass filter, detected by a photomultiplier tube; the signals were acquired by a Boxcar integrator. All of the experiments were carried out at room temperature (295±3 K).

An LIF spectrum demonstrating vibrational excitation of SiO in the reaction of SiH_4+ O(^{1}D) is shown in Fig. 1, where the A–X bands of v'' = 0 to 8 are assigned and a simulation assuming T_v = 5000 K roughly reproduced the observed spectrum. The probe delay was fixed at 20 μs after photolysis while scanning the excitation wavelength. In the employed reactant concentrations of 5 mTorr SiH_4 (1 Torr = 133.322 Pa) and 10 mTorr N_2O in 10 Torr He, the relaxation of SiO vibration was almost negligible (Fig. 2). For detailed analysis of the nascent vibrational distribution, the integrated intensities of the SiO vibrational bands were converted into relative vibrational populations by using the reported SiO (A–X) Franck–Condon factors[8] and wavelength-dependent sensitivity of the detection system. After making corrections for any overlapping of the minor different vibrational peaks in the observed bands, the result of this procedure was well approximated by a Boltzmann distribution with a vibrational temperature (T_v) of 5200±660 K (2× standard deviation).

Present address: Institut für Physicalische Chemie, Universität Göttingen, Tammannstr. 6, D-37077 Göttingen, Germany.

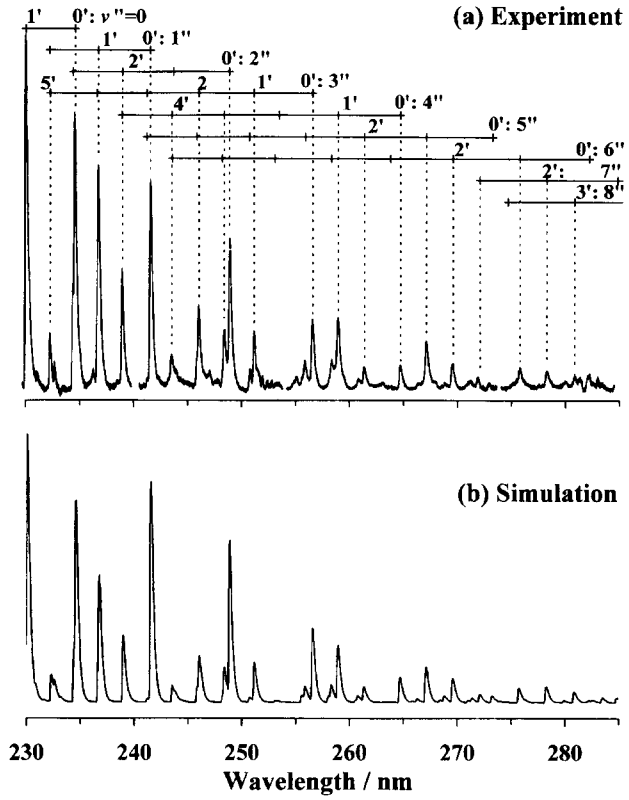

Fig. 1. (a) An example of the LIF spectrum of SiO-($A^1\Pi$–$X^1\Sigma^+$) (v'–v'') showing vibrational excitation in the reaction of SiH_4 with $O(^1D)$. Probe delay is set at 20 μs after ArF laser photolysis of 5 mTorr SiH_4 and 10 mTorr N_2O mixture diluted in 10 Torr He. (b) Numerical simulation of SiO(A–X) spectrum assuming T_v = 5000 K, T_R = 300 K, and 4 cm^{-1} of spectral resolution.

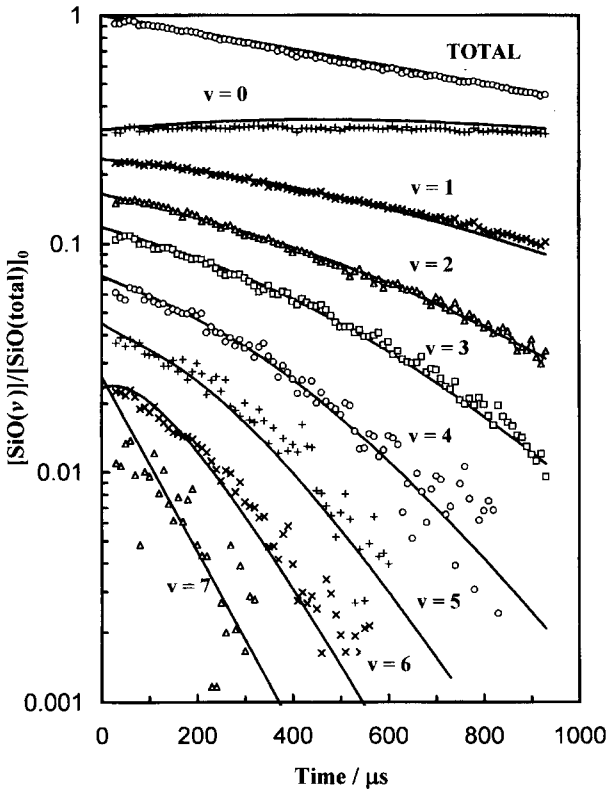

Fig. 2. Relaxation profiles of SiO(v) at 5 mTorr SiH_4 and 10 mTorr N_2O in 10 Torr He. Symbols are the experimental data and solid curves are the calculated profiles using the VET rates obtained by the analysis described in the text. Top trace is the total sum of SiO (v = 0—7) exhibiting first order decay due to diffusion.

Results and Discussion

A. State-Specific Vibrational Transition Rates. Time-dependent intensity profiles of the assigned vibrational states were obtained by scanning the pump-probe delay over the range 0—1 ms, where the probe wavelength was fixed at a selected peak of each vibrational band, as described in Table 1. These bands were chosen so as to avoid any overlapping of different vibrational bands of strong intensities. Profiles of $v'' \geq 1$ show monotonic decay after a fast initial rise due to $SiH_4 + O(^1D)$ reaction. These decay profiles exhibit slight deviations from single exponential ones. On the other hand, the profile of v'' = 0 appears to be rather flat, having a slow rise and decay profile. When profiles of all of the observed levels, i.e. those of v'' = 0—7, are normalized according to the nascent distribution, the total sum shows a monotonic decrease very well approximated by a single exponential decay at a time constant of ca. 850 μs. This decay rate was found to be constant against a change of the concentrations in SiH_4 and N_2O, as long as the pressure of the buffer gas (10 Torr He) was kept constant. This indicates that the reactions of SiO with SiH_4 and/or N_2O are totally negligible. In addition, the reactions of SiO with some minor byproducts, such as OH and H, or with SiO, itself, can be neglected within this period considering that they are at most in the order of 10^{11} molecule·cm^{-3}. Consequently, the observed total SiO decay is entirely attributed to diffusion loss. From gas kinetic theory, the bilateral diffusion coefficient of SiO–He at 10 Torr, 300 K is estimated to be $D = 7 \times 10^{-4}$ m^2 s^{-1}. The decay time constant of the cylindrical diffusion is $\tau = R^2/4D$, where R is the initial radius of the diffusing matter. Giving R = 2 mm as the radius of the photolysis beam in the cell, τ is estimated to be 1.4 ms, which is in reasonable agreement with the current observation.

In order to extract individual transfer rates of each vibrational state from the observed relaxation profiles, the following points are assumed: firstly; only a single quantum

Table 1. Monitored Vibrational Bands of SiO for Analyzing VET Rate

Vibrational bands	Wavelength /nm
1′ - 0″	230.06
0′ - 1″	241.57
0′ - 2″	248.88
0′ - 3″	256.58
0′ - 4″	264.72
2′ - 5″	261.38
2′ - 6″	269.59
2′ - 7″	278.27

downward transition is dominant, i.e., $\Delta v = -1$; secondly, the diffusion loss can be treated as a first-order decay process, and the diffusion rate constant is common for all of the observed vibrational levels at a certain sample mixture composition.

Regarding the first assumption, the single quantum relaxation ($\Delta v = \pm 1$) rule is assured theoretically for the weak collision of harmonic oscilators,[3] and has been supported experimentally as a good approximation for real molecules having anharmonisity. An exceptional case is a multi-quantum resonant V–V transfer, e.g., transition of ($\Delta v = -2$ of O_2 takes place due to the resonance with v_3 of CO_2 at around $v = 18$,[1] which is not the case for this study. The upward transition ($\Delta v = +1$) can be neglected in the current conditions, considering the detailed balance rule; $R_{v\rightarrow v+1}/R_{v+1\rightarrow v} = \exp(-\Delta E_v/k_B T)$.

The relaxation equations for the individual vibrational levels are then expressed by,

$$\frac{d}{dt}X_0 = R_1 X_1 - R_d X_0, \quad (1)$$

$$\frac{d}{dt}X_v = R_{v+1}X_{v+1} - R_v X_v - R_d X_v, \quad (v \geq 1) \quad (2)$$

where, X_v is the concentration of v th vibrational state, R_v is the first-order transition rate constant from v to $v-1$, and R_d is the diffusion-loss rate constant. Once R_d is given, one can obtain a simulated profile of X_0 by a numerical integration of Eq. 1 using the observed X_1 and X_0 profiles. Since R_1 is the only unknown parameter in Eq. 1, it can be determined so that the input X_0 and the output X_0 are self-consistent. R_2 can be determined as well by integrating Eq. 2 using the experimental X_2 and X_1 along with the previously determined R_1. In this way, the R_v's were determined successively up to $v = 6$.

In addition, a reversed approach to the above was conducted. Namely, at the first step, R_7 was determined by fitting the X_7 profile while neglecting any contribution from $v = 8$. The next step was to determine R_6 by fitting X_6 with given X_7, X_6, and R_7. By repeating these steps, the R_v's were determined successively down to $v = 1$. The resultant R_v's were in reasonable agreement in the range $v = 1$ to 5. A result of this fitting procedure is exhibited in Fig. 2.

N_2O is found to be an effective collider for the relaxation of SiO(v) in the employed compositions. The first-order rates clearly showed a linear dependence on the N_2O concentration at all vibrational levels, as shown in Fig. 3. Consequently, the second-order VET rate constants in collisions with N_2O were determined from the slopes in the plot against the N_2O concentration. The results are shown in Fig. 4. Apparently, it is not a standard linear function of v, but one having a maximum at $v = 2$ or 3. The reason for this is further discussed in the next section.

The intercepts in Fig. 3 should consist of contributions from He and SiH_4 exclusively, since the diffusion-loss terms assessed in the above analysis have already been eliminated. The contributions of SiH_4 were examined by increasing the SiH_4 concentration up to 20 mTorr and were found to be less than 10% within the intercepts at the standard compositions, including 5 mTorr SiH_4, which do not exceed the error limits of the intercepts. Hence, we ascribed all VET rates at the intercept to those of collisions with He. The resultant rate

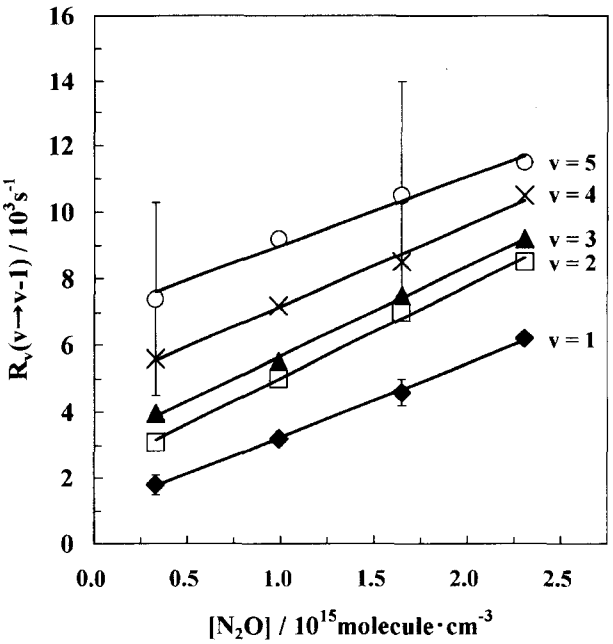

Fig. 3. First-order vibrational relaxation rates of SiO(v) as a function of N_2O concentration. [SiH_4] = 5 mTorr, P_{total} = 10 Torr He. Error limits were estimated by setting R_7 as 0 and double the best fit value in the initial guess of the fitting procedure (see text). Typical error bars at $v = 1$ and $v = 5$ are indicated.

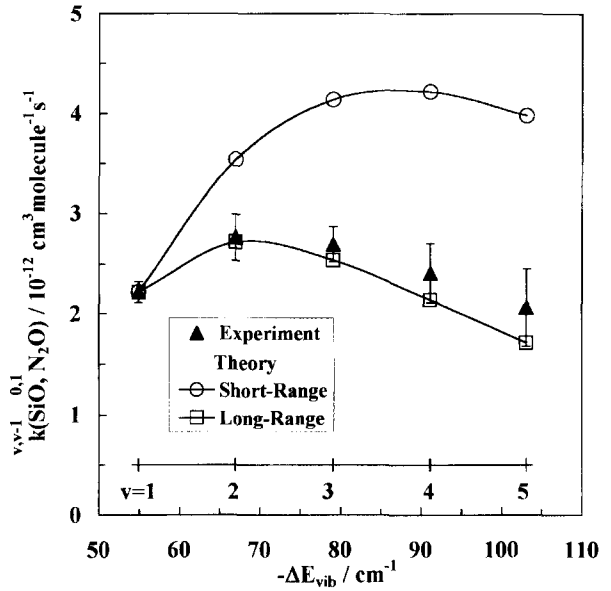

Fig. 4. Second-order V–V transfer rate constants of SiO(v) in collisions with N_2O as a function of energy gap. Solid triangles are the experimental data points and open symbols are calculated by V–V energy transfer theories. The vertical scales of the short-range theory and the long-range theory were multiplied by 96.1 and 0.0198, respectively, to adjust them to the experiment at $v = 1$.

constants are shown in Fig. 5 and summarized in Table 2 together with those by N_2O.

B. The Mechanism of Vibrational Relaxation. In the current evaluation, the transition rates of SiO(v) in collisions with N_2O are about two orders of magnitude larger than those with He. Theoretically, vibration-to-translation (V–T) and vibration-to-vibration (V–V) transfer concepts have been acknowledged as two principal mechanisms of VET.[3]

In the case of an SiO–He collision, the V–T process is the only possible mechanism. The vibrational transition probability upon a neutral atom–molecule collision has been frequently compared with the SSH theory,[9] which has been known to suitably predict the temperature dependence and mass effect for the VET rate. Here, a thermally averaged expression of the SSH theory was applied to the He–SiO system using $\varepsilon_{\text{He–SiO}} = 56.5$ K and $r_{0\ \text{He–SiO}} = 3.59$ Å as the L–J parameters.[11] SSH theory gives a $v = 1 \rightarrow 0$ transition probability per collision, P_{10} of ca. 10^{-4}, which is an order of magnitude larger than the observed one. Nonetheless, this seems to be an acceptable deviation, since the same is true for other molecules, like CO, in the room-temperature region.[3] The v dependence is dominated by the matrix-element term, approximated by the Landau–Teller relation:

$$Q_{jf}{}^2 \propto (j + 1/2 \pm 1/2)\delta_{fj\pm1}, \tag{3}$$

where Q_{jf} is the matrix element for the j–f transition, and δ_{ik} is the Kronecker's delta. The small deviation from linearity on v is ascribed to the term $\exp(-2\pi\omega_{v,v-1}l/v)$, where the transition frequency, $\omega_{v,v-1}$, is gradually decreasing with v. Finally, the rate constants calculated by the SSH theory were adjusted by setting the steric factor so that the magnitude of second-order T–V rate constant $k_{10}{}^{\text{TV}}$ agrees with the measured rate constants; only the dependence on v is examined in this paper. As shown in Fig. 5, the calculated v dependence is in good agreement with the experimental one.

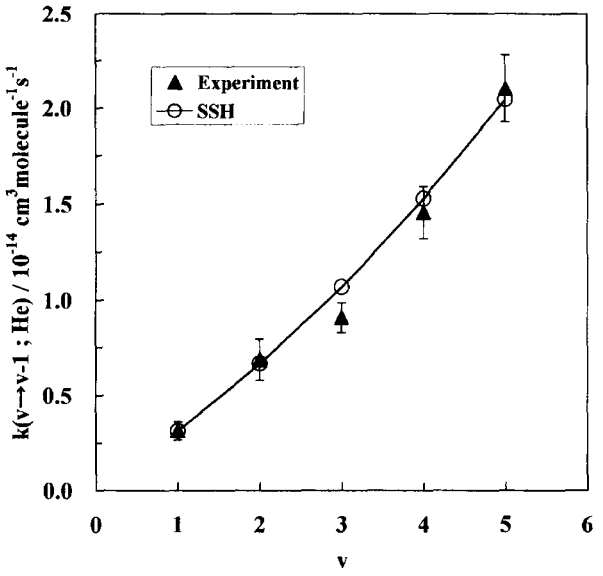

Fig. 5. Second-order vibrational transition rate constants of SiO(v) in collisions with He. Solid triangles are the experimental data points and open symbols are the calculated ones by the SSH theory. The vertical scale of SSH(A) was multiplied by 0.084 to adjust the point to the experiment at $v = 1$.

Upon a N_2O–SiO collision, the V–V transfer mechanism is supposed to dominate, since N_2O has a 1285 cm^{-1} of asymmetric stretch mode, which is close to 1230 cm^{-1} of the SiO fundamental frequency. The short-range interaction theory of Rapp[12] and the long-range dipole–dipole interaction theory of Sharma and Brau[13] have been tested for numerical evaluations of the second-order V–V transition rate constants of the SiO–N_2O collision, k^{VV} ($\text{SiO}^{v,v-1}$, $\text{N}_2\text{O}^{0,1}$) with L–J parameters of $r_{\text{SiO–N}_2\text{O}} = 4.22$ Å and $\varepsilon_{\text{SiO–N}_2\text{O}} = 569.3$ K. Here, again, only the relative magnitude of the rate is examined by shifting the theoretical results so that k^{VV} ($\text{SiO}^{1,0}$, $\text{N}_2\text{O}^{0,1}$) agrees with the experimental result. The calculated results are compared with the experiment in Fig. 4. As shown in the figure, the results of long-range theory are in better agreement with the observed rates in terms of the v dependence than those of the short-range theory. Since the Landau–Teller relations in the matrix elements are the same between the theories, the difference should come from a factor involving the energy gap, $\Delta E = E_{1,0}{}^{\text{N}_2\text{O}} - E_{v,v-1}{}^{\text{SiO}}$.

The short-range V–V theory has been constructed with a similar concept of V–T transfer, in that an exponential repulsive interaction between closest atoms is responsible for the transition. The dominant term for the energy-gap dependence is

$$P_{jf}{}^{\text{SR}} \propto \text{sech}^2\left(\frac{2L\Delta\omega}{u}\right), \tag{4}$$

where L is the characteristic length of the repulsive potential, $\Delta\omega$ is the energy gap in the angular frequency unit and u is the collision velocity. In many cases L has a value close to

Table 2. Second Order VET Rate Constants $k(\text{SiO}^{v\rightarrow v-1}\text{–X})$ for X = He and N_2O[a)]

v	V–T rate for SiO–He collision $k^{\text{VT}}_{v,v-1}$	V–V rate for SiO–N_2O collision k^{VV} ($\text{SiO}^{v,v-1}$–$\text{N}_2\text{O}^{0,1}$)
1	3.1±0.4	2.2±0.1
2	6.9±1.2	2.7±0.3
3	9.2±0.8	2.6±0.2
4	14.2±1.2	2.3±0.4
5	21.0±2.4	2.1±0.5
Unit	10^{-15} cm^3 $molecule^{-1}$ s^{-1}	$10^{-12}cm^3$ $molecule^{-1}$ s^{-1}

a) Error limits are statistical 2σ.

0.2 Å.

On the other hand, a long-range theory has been established under the assumption that the dominant interaction is the dipole–dipole potential, expressed as $V = Cr^{-3}$, where r is the molecule–molecule distance. The energy-gap dependence in this case is given by

$$P_{jf}^{LR} \propto \Delta\omega \exp\left(-\frac{2d\Delta\omega}{u}\right), \quad (5)$$

where d is the collision diameter, frequently being given as equivalent to the L–J r parameter. Apparently P_{jf}^{LR} is a stronger function of $\Delta\omega$ than P_{jf}^{SR}.

The VET rates of CO seems to be a good reference to be compared with the current results for SiO, because CO is the carbon analog to SiO and its VET rates have been extensively studied. Figure 6 shows the V–V transfer probabilities of CO with various colliders, summarized by Hancock and Smith[4] as a function of the energy gap along with the current results for SiO–N_2O. The SiO results are found to be within the scattered range of the CO probabilities, and the slope against ΔE is close to the entire slope for CO. The absolute probabilities for SiO were expected to be above those of CO, since the dipole moment of SiO is 30-times larger than that of CO.[10] The long-range V–V probability is supposed to be proportional to the dipole moment of both colliders. Although the cause of the inconsistency in terms of the magnitude of dipole moment is not apparent, approximations involved in the theories, such as neglecting the molecular orientation, should be properly included so as to improve the theoretical estimations.

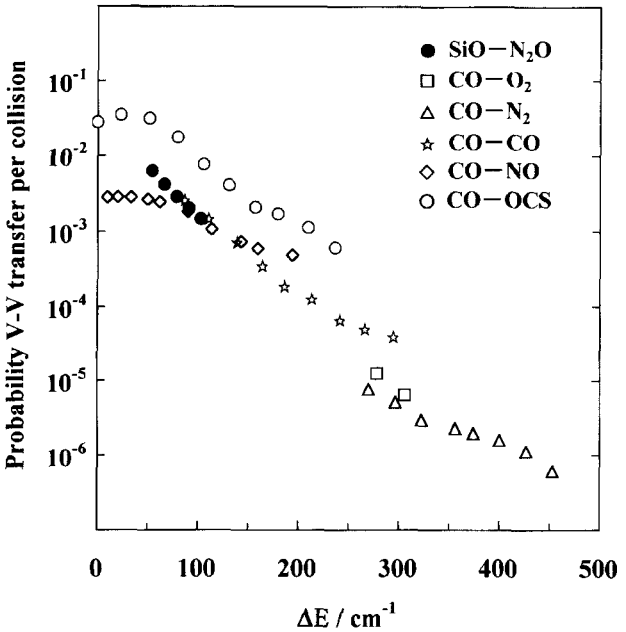

Fig. 6. Probabilities of V–V transfer of $CO_{v,v-1}$–$X_{0,1}$ and $SiO_{v,v-1}$–$N_2O_{0,1}$ as a function of energy gap. According to the procedure of Hancock et. al. Here, all the probabilities of exothermic transition divided by v are exhibited.

Conclusions

In the present study, a chemical-excitation scheme has been effectively used to analyze the state-resolved vibrational energy transfer of SiO for the first time. The results demonstrated a clear contrast between the V–T transfer mechanism of the SiO–He collision and the near-resonant V–V transfer mechanism of the SiO–N_2O collision in terms of the v dependence as well as the magnitudes of the VET rate constants. That is, relatively ineffective VET rates of SiO(v) vs. He showed an approximately linear dependence on v, which is well represented by the Landau–Teller relation essentially included in the SSH theory. On the other hand, the increasing energy gap on v was found to be responsible for the nonlinear v dependence for the SiO–N_2O collision, which is suitably reproduced by the long-range V–V theory of Sharma and Brau.

Appendix

A1 V–T Energy Transfer Rates. The probability of a vibration-to-translation energy transfer upon collisions of atom A into molecule BC is considered. Under the assumption that the repulsive potential between A and B is $V_R(r) = V_0\exp(-r/L)$, the quasi-classical, one-dimensional transition probability is given by Schwartz, Slawsky, and Herzfeld[3,9] as below:

$$P(u)_{i\to i\pm1} = \left(\frac{8\pi\mu\omega L^2}{h}\right)^2 \left(\frac{m_C}{m_{BC}}\right)^2 \frac{Y_{ij}^2}{L^2} \exp\left[-\frac{2\pi L\omega}{u}\left(1 \pm \frac{2\pi h\omega}{2\mu u^2}\right)\right], \quad (A1)$$

where μ is the reduced mass of the A–BC system, ω is the angular frequency of the molecular vibration, Y_{ij} is the vibrational matrix element, and u is the relative velocity between A and BC. The thermal energy-transfer rate is obtained by properly integrating this equation over the three-dimensional collision velocity distribution.

The integration is conducted by an expansion around the most effective velocity, $u_m = (\omega LkT/\mu)^{1/3}$, which gives a consequent SSH expression of the V–T probabilities, written as:

$$P_{i\to i+1} = iP_{1\to0}, \quad (A2)$$

$$P_{i\to i-1} = (i+1)P_{1\to0}\exp(-2\pi h\omega/kT), \quad (A3)$$

$$P_{1\to0} = (Z_0Z_VZ_T)^{-1}, \quad (A4)$$

where

$$Z_V^{-1} = \frac{1}{2}\frac{m_B^2+m_C^2}{m_Bm_C}\frac{m_A}{m_A+m_B+m_C}2\pi^2\frac{\theta}{\theta'}, \quad (A5)$$

$$Z_T^{-1} = \left(\frac{2}{3\pi^3}\right)^{1/2}\left(\frac{\theta'}{\theta}\right)^2\left(\frac{\theta'}{T}\right)^{1/6}\exp\left[-\frac{3}{2}\left(\frac{\theta'}{T}\right)^{1/3}+\frac{\theta}{2T}\right], \quad (A6)$$

$$Z_0^{-1} = \overline{(\cos^2\phi)} = \frac{1}{3}, \quad (A7)$$

$$\theta = \hbar\omega/k = 1.44v, \quad (A8)$$

$$\theta' = \varepsilon'/k = 0.8153\tilde{M}\theta^2L^2, \quad (A9)$$

$$\varepsilon' = \mu(\pi^2\omega L)^2, \quad (A10)$$

$\tilde{M}$ is the reduced mass of the collisional system in atomic units. In order to apply the parameters of the Leonard–Jones potential,

$$V_{LJ} = 4\varepsilon\left[\left(\frac{r_0}{r}\right)^{12} - \left(\frac{r_0}{r}\right)^{6}\right], \tag{A11}$$

L should be determined by matching the repulsive potential with V_{LJ}. There are two methods (A and B) of the matching proposed by SSH.

In method A, L is given so that $V_{LJ} = V_R$ and $dV_{LJ}/dr = dV_R/dr$ at the distance of the closest approach, r_c, in a collision with the relative kinetic energy, $E_m = \mu u_m^2/2$:

$$\left(\frac{r_0}{r_c}\right)^6 = \frac{1}{2}\left[1 + \left(\frac{E_m}{\varepsilon} + 1\right)^{1/2}\right], \tag{A12}$$

yielding

$$\frac{r_0}{L} = 12\left[\frac{1}{2}\left(1 + \sqrt{\frac{E_m}{\varepsilon} + 1}\right)\right]^{1/6}\left[1 + \left(\frac{E_m}{\varepsilon} + 1\right)^{-1/2}\right]. \tag{A13}$$

Method B matches the two potentials at $r = r_c$ and $r = r_0$, which yields:

$$\frac{r_0}{L} = \left[\ln\left(\frac{E_m}{\varepsilon} + 1\right)\right]\left\{1 - \left[\frac{1}{2}\left(1 + \sqrt{\frac{E_m}{\varepsilon} + 1}\right)\right]^{-1/6}\right\}^{-1}. \tag{A14}$$

The value of L is usually around 0.2 Å. Herzfeld and Litovits[14] have modified the transition-probability equation for the LJ potential as:

$$P_{1,0}^{-1} = 1.017\left(\frac{r_0}{r_c}\right)^2 \Omega(2,2)\exp\left(-\frac{\varepsilon}{kT}\right) Z_0 Z_V Z_T, \tag{A15}$$

and the rate constant is given as $k(n) = zP_{n,n-1}$, where the collision frequency is

$$z = 1.017 r_0^2 \Omega(2,2)(8\pi kT/\mu)^{1/2} \tag{A16}$$

and $\Omega(2,2)$ is the Sutherland's correction,[15] which is expressed as

$$\Omega(2,2) = 0.76\left(1 + 1.1\frac{\varepsilon}{kT}\right). \tag{A17}$$

The parameters for the calculations of SiO–He collisions are summarized in Table A1 and the calculated transition probabilities are given in Table A2. For the intermolecular-potential parameters, the following relations are used:

$$r_0 = (r_{0He} + r_{0SiO})/2, \tag{A18}$$

$$\varepsilon = (\varepsilon_{He}\varepsilon_{SiO})^{1/2}. \tag{A19}$$

Table A1. Parameters Used in the Calculations on V–T Energy Transfer for the SiO–He Collision

Species	M / g mol^{-1}	ν / cm^{-1}	θ / K	ε/k / K	r_0 / Å
SiO	44.09	1230.03	1769.8	312	4.6
He	4.003	—	—	10.22	2.576

Table A2. Probabilities for V–T Energy Transfer of SiO–He Collision at 300 K[a)]

Method	L / Å	E_m/ε	$P_{1,0}$	$P_{2,1}$	$P_{3,2}$	$P_{4,3}$	$P_{5,4}$
SSH (A)	0.208	29.3	7.48	16.0	25.6	36.6	48.9
SSH (B)	0.187	27.4	18.0	38.2	61.0	86.5	115

a) $P_{n,n-1}$ values are in unit 10^{-5}.

A2 V–V Transfer Rates. Rapp's Short Range Theory.[12] A collinear encounter of a molecule CB with a molecule AD is considered. Each molecule is assumed to be a harmonic oscillator. As in V–T theory, an exponential repulsive interaction between only end atoms B and A is assumed. Utilizing the Born approximation, the transition probability between the initial state, $\psi_i = \psi_j(Q_{BC})\psi_k(Q_{AD})$, and final state, $\psi_f = \psi_l(Q_{BC})\psi_m(Q_{AD})$, at collision velocity u is expressed as

$$\langle\langle P\rangle\rangle = \frac{4L^2\mu^2|U_{if}|^2}{\hbar^2}\frac{\mu}{kT}\int u^3\exp\left(-\frac{\mu u^2}{2kT}\right)\mathrm{sech}^2\left(\frac{2L\Delta\omega}{u}\right)du, \tag{A20}$$

where $\Delta v = v_i - v_f = \hbar^{-1}(E_j + E_k - E_l - E_m)$ and U_{if} is the vibrational matrix element. L is determined by the same method as in the previous section, and method A is used here. Equation A20 can be integrated approximately by an expansion around the effective velocity, given as $u^* = (3kT/\mu)^{1/2}$, while neglecting the u dependence in the sech term, giving

$$\langle\langle P\rangle\rangle \cong \frac{8L^2|U_{if}|^2}{\hbar^2}\mu kT\,\mathrm{sech}^2\left[2L\Delta v\left(\frac{\mu}{3kT}\right)^{1/2}\right]\exp\left(\frac{\hbar\Delta\omega}{2kT}\right). \tag{A21}$$

The vibrational matrix element at a special case where $l = j-1$ and $m = k+1$ is expressed as

$$|U_{if}|^2 = \left(\frac{CD}{(B+C)(A+D)AB}\right)\frac{j(k+1)\hbar^2}{4\omega_1\omega_2 L^4}. \tag{A22}$$

Long-Range Dipole–Dipole Interaction Theory.[13,16] The angular-averaged interaction potential between two dipoles valid at a large distance r is written as

$$V_{if} = C/r(t)^3,$$
$$C = \frac{1}{3}(\mu_1)_{if}(\mu_2)_{if} = \frac{1}{3}\frac{\mu_1\mu_2}{4\pi\varepsilon_0}, \tag{A23}$$

where μ_1 and μ_2 are the electric dipole moments. The transition probability is obtained by solving the wave equation containing the interaction trajectory as a perturbation. The Sharma–Brau expression[13] of the transition probability integrated over the impact parameter is

$$\langle\langle P\rangle\rangle = \frac{2\pi^2 C^2\Delta\omega\mu}{\hbar^2 d^3 u^*\pi\langle u\rangle kT}\int_0^\infty \exp\left(-\frac{\mu v^2}{2kT}\right)\exp\left(-\frac{2d\Delta v}{u}\right)du, \tag{A24}$$

Table A3. Parameters Used in the Calculations on Vibrational Energy Exchanges of the SiO–N_2O Collision

Molecule	M/g mol^{-1}	ν/cm^{-1}	θ/K	ε/k / K	r_0/Å	μ/D
SiO	44.09	1230.03	1769.8	312	4.6	3.098
N_2O	44.02	1284.9	1848.7	232.4	3.83	0.161

$d = r_{SiO-N_2O} = 4.22$ Å, $\varepsilon_{SiO-N_2O} = 269.3$ K, $C = 1.66\times10^{-37}$ erg cm^3, 1 D $= 3.3564\times10^{-30}$ C m.

Table A4. V–V Energy Transfer Probabilities of SiO-(1→0)–$N_2O(\nu_3{:}0\rightarrow1)$ at 300 K

	$P_{1,0}$	$P_{2,1}$	$P_{3,2}$	$P_{4,3}$	$P_{5,4}$	Unit
Short-range:	5.02	8.02	9.38	9.56	9.02	$\times10^{-5}$
Long-range:	2.42	2.97	2.77	2.34	1.88	$\times10^{-1}$

where d is the hard-sphere collision diameter and $u^* = (2d\Delta\omega kT/\mu)^{1/3}$ is the velocity which maximizes the probability. Equation A24 can be integrated by an expansion around u^* to give

$$\langle\langle P\rangle\rangle = \frac{2\pi^2 C^2 \Delta\omega\mu}{\hbar^2 d^3 u^* kT}\left(\frac{1}{12}\right)^{1/2}\exp\left(-\frac{\mu u^{*2}}{2kT}\right). \quad \text{(A25)}$$

The V–V transfer for SiO(v: $1\rightarrow 0$) with N_2O(v_3: $0\rightarrow 1$) is calculated using the above mentioned theories. The parameters used are given in Table A3, and the calculated results are listed in Table A4.

References

1 G. W. Flynn, C. S. Parmenter, and A. M. Wodtke, *J. Phys. Chem.*, **100**, 12817 (1996).

2 X. Yang, J. M. Price, J. A. Mack, G. G. Morgan, C. A. Rogaski, D. McGuire, E. H. Kim, and A. M. Wodtke, *J. Phys. Chem.*, **97**, 3944 (1993).

3 J. T. Yardley, in "Introduction to Molecular Energy Transfer," Academic Press, New York (1980).

4 G. Hancock and I. W. M. Smith, *Appl. Optics*, **10**, 1827 (1971).

5 A. D. Sappey and R. A. Copeland, *J. Chem. Phys.*, **93**, 5741 (1990).

6 K. Okuda, K. Yunoki, T. Oguchi, Y. Murakami, A. Tezaki, M. Koshi, and H. Matsui, *J. Phys. Chem.*, **A101**, 2365 (1997).

7 A. Takahara, A. Tezaki, and H. Matsui, *J. Phys. Chem.*, **103**, 11315 (1999).

8 H. S. Liszt and W. H. Smith, *J. Quant. Spectrosc. Radiat. Transfer*, **12**, 947 (1972).

9 R. N. Schwartz, Z. I. Slawsky, and K. F. Herzfeld, *J. Chem. Phys.*, **20**, 1591 (1952).

10 R. N. Schwartz and K. F. Herzfeld, *J. Chem. Phys.*, **22**, 767 (1954).

11 D. R. Lide, "CRC Handbook of Chem. and Phys.," 73rd ed, CRC Press, 1992.

12 D. Rapp, *J. Chem. Phys.*, **43**, 316 (1965).

13 R. D. Sharma and C. A. Brau, *J. Chem. Phys.*, **50**, 924 (1969).

14 K. F. Herzfeld and T. A. Litovitz, "Absorption and Dispersion of Ultrasonic Waves," Academic Press, New York (1959).

15 J. O. Hirschfelder, C. F. Curtiss, and R. B. Bird, "Molecular Theory of Gases and Liquids," Wiley, New York (1954).

16 J. T. Yardley, *J. Chem. Phys.*, **50**, 2464 (1969).